Virology 433 (2012) 462–470

Contents lists available at SciVerse ScienceDirect

Virology

journal homepage: www.elsevier.com/locate/yviro

The specific infectivity of hepatitis C virus changes through its life cycle

Sun Ju Keum [a], Sung Mi Park [a], Ji Hoon Park [a], Jong Ha Jung [a], Eun Ji Shin [a], Sung Key Jang [a,b,c,*]

[a] Department of Life Science, POSTECH Biotech Center, Pohang University of Science and Technology, Pohang, South Korea
[b] Division of Integrative Biosciences and Biotechnology, Pohang University of Science and Technology, Pohang, South Korea
[c] Biotechnology Research Center, Pohang University of Science and Technology, Pohang, South Korea

ARTICLE INFO

Article history:
Received 11 June 2012
Returned to author for revisions
6 July 2012
Accepted 29 August 2012
Available online 19 September 2012

Keywords:
Hepatitis C virus
One-step growth
The kinetics of HCV replication
The kinetics of HCV production
Chracterization of HCV particles
Specific infectivity of HCV

ABSTRACT

Hepatitis C virus (HCV) causes liver diseases, such as hepatitis, liver cirrhosis, steatosis, and hepatocellular carcinoma. To understand the life cycle and pathogenesis of HCV, the one-step growth of HCV in a cell culture system was analyzed using a highly infectious variant of the JFH1 clone. The observed profiles of HCV RNA replication indicated that the synthesis of negative-strand RNAs occurred at 6 h (h) after infection, followed by the active synthesis of positive-strand RNAs. Our measurements of infectious virus production showed that the latent period of HCV was about 12 h. The specific infectivity of HCV particles (focus-forming unit per viral RNA molecule) secreted to the extracellular milieu early in infection was about 30-fold higher than that secreted later during infection. The buoyant densities of the infectious virion particles differed with the duration of infection, indicating changes in the compositions of the virion particles.

Introduction

Over 170 million people worldwide are chronically infected with hepatitis C virus (HCV), which is associated with hepatitis, progressive hepatic fibrosis, liver cirrhosis, and hepatocellular carcinoma (Liang et al., 1993; Wasley and Alter, 2000).

HCV is a member of the *Flaviviridae* family of enveloped, positive-strand RNA viruses (Bartenschlager and Lohmann, 2001). Its genome consists of a single-strand RNA molecule of approximately 9.6 kb, which contains a large open reading frame flanked by 5′ and 3′ untranslated regions (UTRs). The viral RNA is translated into a single large polyprotein of 3010-3040 amino acids, which is co- and/or post-translationally processed by cellular and viral proteases into a number of mature viral proteins.

The replication steps of HCV have been investigated using HCV replicons (Lohmann et al., 1999). Detailed stoichiometric analyses of HCV RNA replication, carried out using crude replicase complexes prepared from lysates of HCV subgenomic or full-length replicons (Aizaki et al., 2004; Ali et al., 2002; El-Hage and Luo, 2003; Hardy et al., 2003; Lai et al., 2003; Quinkert et al., 2005), have indicated that each cell harboring the full-length HCV genome or subgenomic replicon contains approximately 100 negative-strand RNAs, 1000 positive-strand RNAs, and 100,000 copies of each viral protein (Quinkert et al., 2005). More recently, the development of the infectious HCV clone, JFH1, and its derivatives has enabled researchers to investigate the entire life cycle of HCV (Lindenbach et al., 2005; Wakita et al., 2005; Zhong et al., 2005). The HCV particles circulating in chronic HCV patients or those produced in vitro showed heterogeneous densities ranging from 1.06 to 1.20 g/ml (Andre et al., 2002; Cai et al., 2005; Lindenbach et al., 2005; Nielsen et al., 2006; Wakita et al., 2005; Zhong et al., 2005). The differences in the densities of virion particles were attributed to the presence or absence of host lipoproteins and antibodies bound to the circulating viral particles (Gastaminza et al., 2010; Hijikata et al., 1993; Pumeechockchai et al., 2002). The animal(chimpanzee)-derived HCV showed lower buoyant density than the cell-derived HCV (Lindenbach et al., 2006). In the case of HCV particles obtained from HCV patients, the density profiles were found to differ by the stage of infection (Carabaich et al., 2005; Pumeechockchai et al., 2002). Moreover, density gradient analyses of viruses cultivated in vitro showed that virion particles with densities of ~1.10 to 1.14 g/ml had the highest specific infectivity (defined herein as focus-forming unit per viral RNA molecule) (Gastaminza et al., 2006; Grove et al., 2008; Lindenbach et al., 2005). An electron cryomicroscopic (cryoEM) analysis revealed two major viral populations of ~60 and ~45 nm in diameter; the ~60-nm particles, which were characterized by a membrane bilayer, showed high specific infectivity (Gastaminza et al., 2010). Recent studies have indicated that infectious virus assembly requires members of the very-low-density-lipoprotein (VLDL) biosynthetic

* Corresponding author at: Department of Life Science, POSTECH Biotech Center, Pohang University of Science and Technology, Pohang, South Korea
E-mail address: sungkey@postech.ac.kr (S. Key Jang).

0042-6822/$ - see front matter © 2012 Elsevier Inc. All rights reserved.
http://dx.doi.org/10.1016/j.virol.2012.08.046

machinery, including apolipoprotein E (apoE) and microsomal transfer protein (Gastaminza et al., 2008; Huang et al., 2007; Nahmias et al., 2008). ApoE, in association with an HCV particle, facilitates viral infection via an interaction with the low-density-lipoprotein receptor (LDLR) (Owen et al., 2009).

Using the in vitro cultivation systems, virus proliferation has been investigated (Lindenbach et al., 2005; Wakita et al., 2005; Zhong et al., 2005). However, the experiments were performed with low multiplicity of infection (moi), which results in ensemble profiles of virus proliferation including several generations of viruses together. The relationship between HCV infectivity and buoyant density of virus particles has been investigated with the mixtures of HCV particles produced at various stages of infection. In other words, characterization of viruses produced at specific stage after infection has not been reported. Moreover, there was no report showing the quantitative changes of positive- and negative-strand HCV RNAs within the first 24 h after infection. In order to investigate the profiles of HCV proliferation during a single infection cycle, experiments with high titer of HCV (5 moi or higher) sufficient for infecting more than 99% of cells are needed.

In this study, we investigated HCV life cycle with high titer of HCV (MOI=5 or 6) using a cell culture–adapted infectious HCV (JFH-m4) harboring adaptive mutations in the E2 and p7 proteins (Kim et al., 2011). When cells are inoculated with 5 MOI, theoretically 99.3% of cells are infected with at least one infectious virion particle. With this approach, we obtained one-step growth curve of HCV since superinfection of HCV does not occur to the HCV-infected cells (Tscherne et al., 2007). With this synchronized infection system, we analyzed the profiles of HCV RNA replication, infectious virus production, and the properties of HCV particles produced during early and late stage after infection.

Results

The ratio of positive- to negative-strand RNA changes as HCV infection proceeds

To obtain a high titer of HCV, we collected a large amount of virus and concentrated virus as described in the Materials and methods section. Core proteins were observed from approximately 95% of cells by immune-staining at 18 h after inoculation of HCV (MOI=5) to Huh7.5.1 cells (data not shown) indicating that viruses were actively proliferating in most of cells. To determine the profiles of HCV RNA replication during HCV infection, Huh7.5.1 cells (4×10^4 cells/well in a 24-well plate)

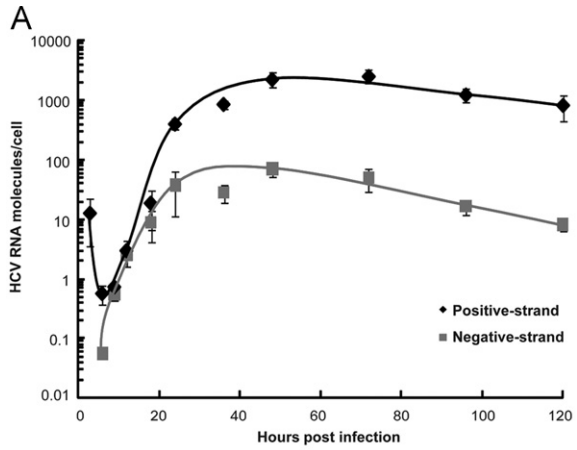

C

Infection times(hrs)	Positive-strand RNA/cell	Negative-strand RNA/cell	Ratio of positive-/negative-strand RNA
3	(12.8±4.9)	under detection limit	
6	(1.0±0.2)	(0.1±0.0)	10.1
9	(1.4±0.2)	(1.4±0.4)	1.0
12	(3.0±1.4)	(2.5±0.2)	1.2
18	(18.9±12.1)	(8.9±4.8)	2.1
24	(404.5±87.7)	(37.4±26.3)	10.8
36	(868.5±135.3)	(28.4±9.4)	30.5
48	(2275.6±632.9)	(70.5±18.9)	32.3
72	(2555.6±649.9)	(50.0±21.1)	51.1
96	(1247.4±299.4)	(16.6±4.5)	75.2
120	(1053.4±495.8)	(10.4±2.6)	101.1

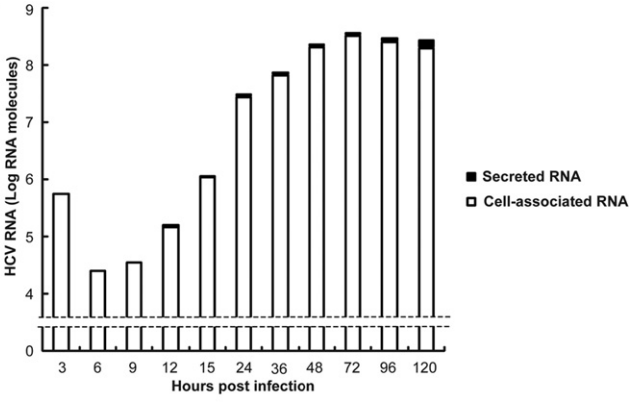

Fig. 1. Analysis of cell-associated and secreted HCV RNAs during the replication cycle. Huh7.5.1 cells were incubated with HCVcc at a MOI of ~6 FFU/cell for 3 h, and then cultivated with complete DMEM. (A) Cell-associated RNAs were extracted from cells at the indicated times, and then the positive- and negative-strand HCV RNAs were quantified using RT-qPCR. The number of HCV RNA molecules per cell was calculated by dividing the number of HCV positive- and negative-strand RNAs by the total cell number at each time point. The mean values and standard deviations obtained from three independent experiments are depicted as dots and bars, respectively. (B) Table summarizing the quantities of positive- and negative-strand HCV RNAs per cell shown in panel (A). The ratios of positive- to negative-strand RNAs are also depicted. The amount of negative-strand RNAs at 3 h pi was under the detection limit. (C) The media of HCV-infected cells were harvested and treated with RNase A (40 μg/ml) for 30 min at 37 °C, as previously described (Gastaminza et al., 2006).The remaining RNAs were purified and quantified by RT-qPCR. (D) The cell-associated and secreted HCV RNAs were purified, and the positive-strand RNAs were quantified. The amounts of secreted RNAs (black columns) are shown on top of the amounts of cell associated RNAs (white columns) to clearly indicate the total amounts of RNA.

were incubated with a high titer of HCV (2×10^5 focus-forming units (FFU) in 300 μl containing 5×10^8 copies of HCV RNA, MOI = 5 FFU/cell) at 37 °C for 3 h, and viral RNAs were isolated from cells and culture supernatants at the times indicated in Fig. 1A and then the amount of HCV RNAs were quantified by qRT-PCR. We confirmed that self and/or false priming events did not occur at the qRT-PCR assays used in the quantification of positive- and negative-sense viral RNAs (Fig. S1). Similar to the findings of previous reports (Lindenbach et al., 2005; Wakita et al., 2005; Zhong et al., 2005) the infectious virus dose per viral RNA molecule (specific infectivity) was approximately 1 out of 1000 RNA molecules. Immediately after the adsorption period of 3 h, we detected 5.5×10^5 copies of positive-strand HCV RNA in the total infected cells, indicating that 1 out of every 1000 copies of positive-strand HCV RNA had entered or associated with cells. The number of positive-strand HCV RNAs subsequently deceased, reaching a minimum average level of 1 positive-strand RNA per cell at 6 h pi (Fig. 1A and B). In contrast, negative-strand HCV RNAs, which serve as the template for the synthesis of new positive-strand HCV RNAs, were first detected at 6 h pi, indicating that the negative-strand HCV RNA was first synthesized at an early stage of RNA replication. This is similar to the case of the yellow fever virus (Lindenbach and Rice, 1997). The amount of positive-strand RNA remained almost the same level between 6 h pi and 9 h pi, whereas the amount of negative-strand RNA increased 14-fold during this period (Fig. 1A and B). Surprisingly, the ratio of positive- to negative-strand RNA was almost 1:1 at 9 h pi. The amounts of both positive- and negative-strand RNAs increased equally from 9 to 12 h pi, indicating that both positive- and negative-strand RNAs were amplified during this stage of infection. Synthesis became biased toward positive-strand RNAs after 12 h pi, with the ratio of positive- to negative-strand RNA eventually reaching about 100:1 at 120 h pi (Fig. 1B). The largest amounts of viral RNA were produced at 48 and 72 h pi, with viral RNA production decreasing gradually thereafter (Fig. 1A and B).

To measure the secretion of HCV RNAs, the amounts of positive-strand HCV RNAs were measured in the cell culture media (Fig. 1C). Unencapsidated HCV RNAs, which could have originated from killed and/or ruptured cells, were removed from the media using RNase A (40 μg/ml), as described in the Materials and methods section. No significant difference in the amounts of HCV RNAs with and without RNase A treatment was observed (data not shown). Secreted HCV RNAs were first detected at 12 h pi, when an average of 1 RNA molecule was secreted per

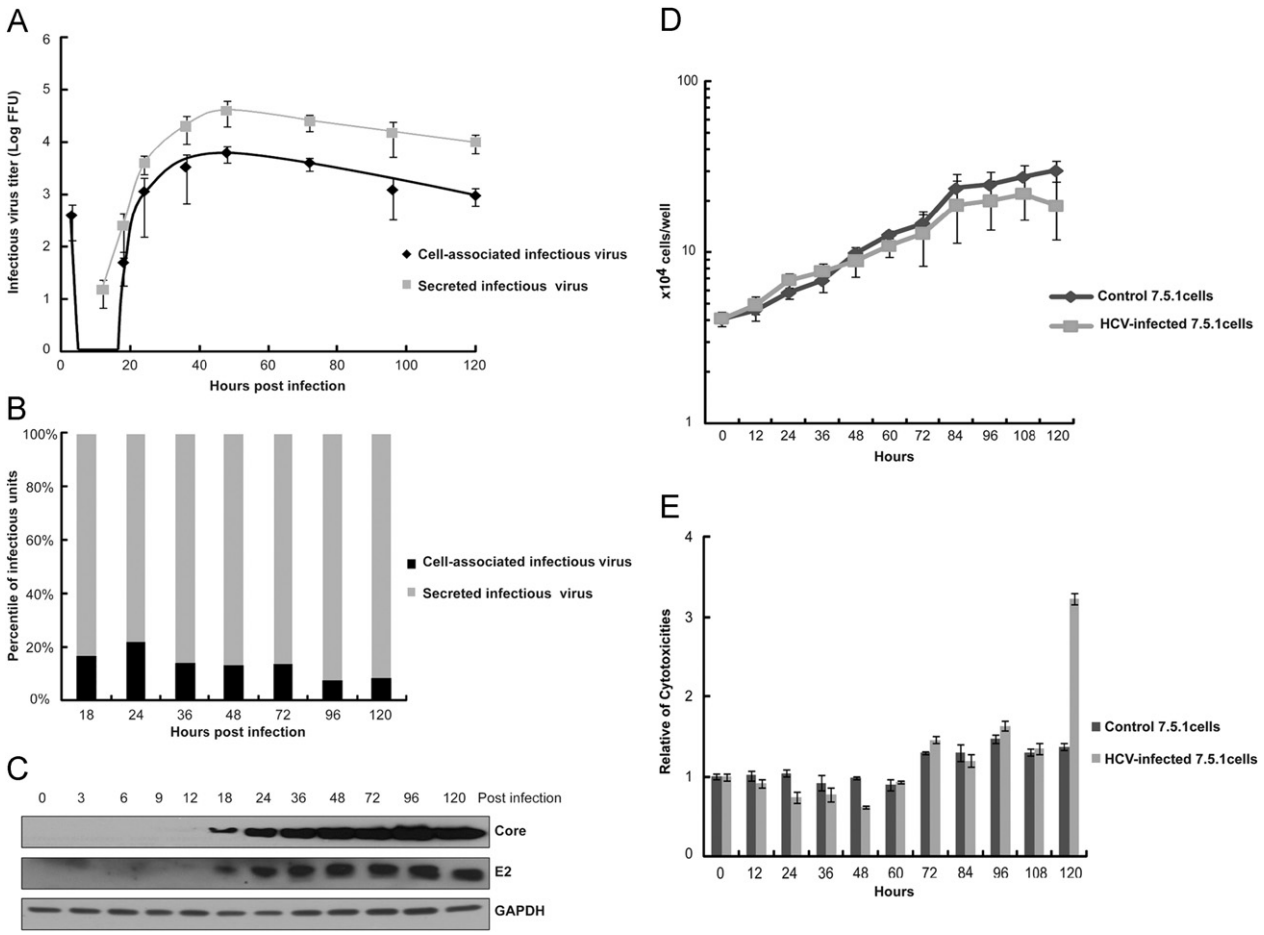

Fig. 2. The kinetics of infectious virus production. (A) Huh7.5.1 cells inoculated with HCVcc at a MOI of ~6 FFU/cell were cultivated for the indicated times, and the culture media and the HCV-infected cells were collected and subjected to measurement of their infectious HCV titers. The infectious virus titers at various stages in the media (secreted viral titer) and in the cell lysates (cell-associated viral titer) were determined by infecting naïve cells. The mean values and standard deviations obtained from three independent experiments are depicted as dots and bars, respectively. (B) The relative amounts of cell-associated (black) and secreted (gray) infectious viruses at various stages after infection are depicted as columns. (C) The levels of viral and host proteins were determined by Western blotting using core-, E2-, and GAPDH-specific antibodies. (D) The effect of HCV infection on cell growth. At the indicated times after infection, HCV-infected cells (gray lines) and uninfected control cells (black lines) were trypsinized at 37 °C for 3 min, and cell numbers were counted using a hemocytometer. The mean values and standard deviations obtained from three independent experiments are depicted as dots and bars, respectively. (E) The viability of HCV-infected and uninfected Huh7.5.1 cells was determined using a ToxiLight bioassay kit. The relative cytotoxicities of samples at various times after infection were determined by setting the luciferase activity in uninfected cells at the starting point = 1. The mean values and standard deviations obtained from three independent experiments are depicted as columns and bars, respectively.

10 cells. At 24 h pi, 1 copy of HCV RNA was secreted per cell, on average. After this stage, the amount of HCV RNAs secreted from cells gradually increased until 120 h pi. To examine the ratios of cell-associated to secreted HCV RNAs, we analyzed the quantities of positive-strand RNAs at the indicated times (Fig. 1C and D). Less than 10% of the HCV RNAs were secreted into the culture media at each time measured. Because the amount of secreted RNAs continually increased while the level of cell-associated HCV RNAs did not, the proportion of secreted RNAs was highest at 120 h pi (Fig. 1C and D). We observed the similar patterns of profiles of cell-associated and secreted HCV RNAs with qRT-PCR using tagged primers to improve strand-specific detection of RNAs (Fig. S2) (Bessaud et al., 2008; Boncristiani et al., 2009; Craggs et al., 2001; Lanford et al., 1995). These results indicate that a small portion of HCV RNAs replicated in cells are secreted into medium.

The majority of mature viruses are secreted into the medium

To determine the kinetics of infectious HCV production, Huh7.5.1 cells (4×10^4 cells/well in a 24-well plate) were infected with a high titer HCV (MOI=5, 2×10^5 focus-forming units (FFU) in 300 μl). After infection, the cell culture media and infected cell lysates were collected at the indicated times (Fig. 2A), and viral titers were measured by the determining the focus-forming units (FFUs) of the samples. Right after the adsorption period of 3 h, 4×10^2 infectious viruses were detected within the total cells. Infectious viruses were not detected in cell lysates at 6–15 h pi. At 18 h pi, newly produced viruses were first detected in the cell lysates (Fig. 2A). The titer of infectious viruses increased up to 48 h pi, when $\sim10^3$ infectious viruses were detected within the infected cells. Secretion of infectious viruses into the culture medium was first detected at 12 h pi, when HCV RNAs were also detected in medium. This indicates that a period of about 12 h pi is required for HCV to be produced. The infectious viral titers peaked at 48 h pi, and then gradually decreased thereafter (Fig. 2A). We next investigated the relative ratios of the cell-associated to secreted infectious viral titers at various times after HCV inoculation (Fig. 2A). The ratio of cell-associated to secreted infectious viral particles reached 20% at 24 h pi, and then gradually decreased to 10% (Fig. 2B).

To examine the relationship between infectious virus production and the level of viral proteins, Western blotting of HCV core and E2 proteins was performed on cell lysates collected at the indicated times (Fig. 2C). The core and E2 proteins were first detected at 18 h pi; they increased until 48 h pi, and plateaued thereafter (Fig. 2C). This indicates that the viral protein levels remain high in infected cells through the late stage of infection.

The effects of HCV infection on the host cells were monitored by counting cell numbers in HCV-infected cultures versus uninfected controls. Huh7.5.1 cells ($\sim3\times10^4$) were seeded and cultivated in 24-well plates for 18 h before infection and then infected with a high titer of HCV (MOI=6). The cell growth kinetics revealed that the cell numbers increased similarly in both cultures until 108 h pi, but the growth rate was slightly lower in HCV-infected cells compared to uninfected controls (Fig. 2D). In HCV-infected cultures, however, the cell number decreased between 108 and 120 h pi, and cytotoxicity, which was monitored by adenylate kinase activity in the medium, was detected at 120 pi (Fig. 2E) (Crouch et al., 1993; Kedmi and

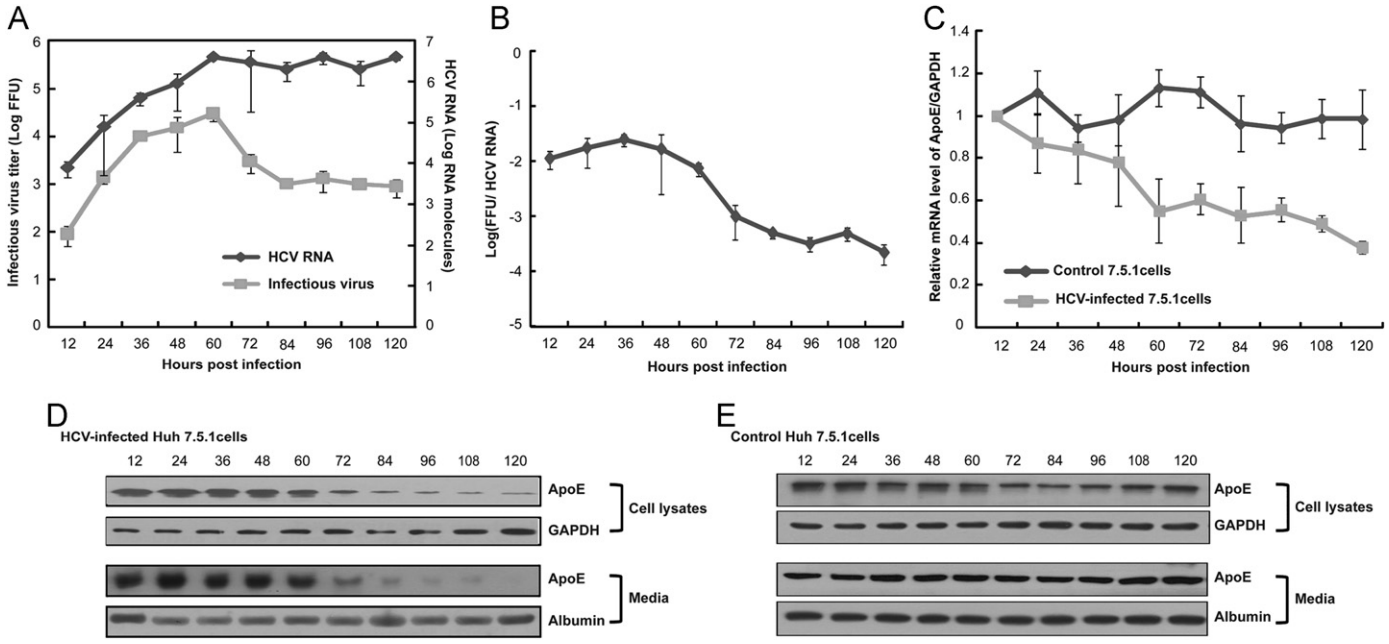

Fig. 3. Changes in specific infectivity and apoE levels during HCV proliferation. Huh7.5.1 cells inoculated with HCVcc at a MOI of ~6 FFU/cell were cultivated with complete DMEM. The culture medium was harvested every 12 h and replaced with fresh medium. (A) The number of HCV RNA molecules (black line) and the infectious virus titer (gray line) in culture media collected at the indicated times were analyzed by RT-qPCR and infectious dose titration, respectively. The mean values and standard deviations obtained from three independent experiments are depicted as dots and bars, respectively. (B) Specific infectivity of HCV in culture media collected at the indicated times after infection. The log values of the infectious virus titer (FFU) divided by the number of HCV RNA molecules at the indicated times are depicted in the graph. The mean values and standard deviations obtained from three independent experiments are depicted as dots and bars, respectively. (C) HCV-infected Huh7.5.1 cells (gray line) and control Huh7.5.1 cells (black line) were collected every 12 h, and the apoE mRNA levels inside cells at the indicated times were determined by RT-qPCR. The level of apoE RNA was normalized by that of GAPDH mRNA, and then relative RNA levels are depicted by setting the RNA level at 12 h pi to 1. The mean values and standard deviations obtained from three independent experiments are depicted as dots and bars, respectively. apoE and GAPDH mRNAs were quantified by using a apoE primers apoE-F(5′-GTTGCTGGTCACATTCCTGG-3′) and apoE-R(5′′-CAGTTGTTCCTCCAGTTCCG-3′) and a GAPDH primers GAPDH-F(5′-CATTGACCTCAACTACATGG-3′) and GAPDH-R(5′-GAGGCAGGGATGATGTTC-3′), respectively. (D) and (E) Huh7.5.1 cells were infected with HCV (D) or left uninfected (E), and cells and media were collected every 12 h. The apoE levels inside cells and culture media obtained at the indicated time were determined by Western blotting using an apoE-specific antibody. The levels of GAPDH and albumin proteins were monitored as controls of housekeeping and secretory proteins, respectively.

Katzenelson, 1978). In other words, the HCV-infected cells did not show serious growth defects for at least 4.5 day (when they were shedding infectious virion particles into the medium), but they eventually succumbed to the virus.

The composition and specific infectivity of HCV co-varies during the course of infection

Although the amount of HCV RNA secreted into the extracellular milieu gradually increased during infection (Fig. 1C), the infectious virion particles secreted into the medium increased until 48 h pi and then gradually decreased thereafter (Fig. 2A). This indicates that the specific infectivity of HCV changed during the course of viral infection. However, it should be noted that the amount of HCV RNA and the infectious units of virion particles were measured using media containing the virion particles that had accumulated up to the indicated time points (Figs. 1 and 2). In order to investigate the properties of virions newly produced within the 12 h prior to collection, culture media were harvested every 12 h and replaced with fresh media. The amount of HCV RNA and infectious virus units in the media were then measured (Fig. 3). The amounts of HCV RNA secreted into the media increased until 60 h pi, and then similar amounts of viral RNAs were secreted until 120 h pi (Fig. 3A). In contrast, the infectious virus titer in the medium increased until 60 h pi and then decreased precipitously until 84 h pi, even though the amounts of secreted viral RNAs remained the same during this period (Fig. 3A). The infectious viral titer was unchanged from 84 h to 120 h pi. These findings indicate that the viral particles produced during the early stage of infection (12–60 h pi) had 10–100 fold higher specific infectivities than those produced during the late stage of infection (72–120 h pi) (Fig. 3B). On average 1 infectious unit per 50–150 viral RNA molecules was observed among viral particles produced between 12 and 60 h pi, whereas 1 infectious unit per 1000–5000 viral RNA molecules was observed after 72 h pi (Fig. 3B). This result indicates that virion particles produced at the early stage of infection were more infectious than virus particles produced at the late stage of infection. In other words, most of the HCV RNAs secreted during the late stage of infection were not infectious.

Previous studies have suggested that apoE is required for the formation of infectious HCV particles, and it is included in the infectious HCV virions (Benga et al., 2010; Chang et al., 2007; Jiang and Luo, 2009). In association with HCV virions, apoE proteins facilitate viral entry through interactions with LDLR and scavenger receptor class B member I (SR-BI) (Chang et al., 2007; Hishiki et al., 2010; Jiang and Luo, 2009). Thus, we investigated the role of apoE in HCV infection by monitoring the amounts of apoE mRNA and protein in HCV-infected cells and the amount of apoE protein secreted into HCV-infected culture media (Fig. 3C and D). To observe newly secreted apoE proteins, HCV-infected cells were subjected to medium changes every 12 h, and the harvested media were assessed for apoE. The amount of apoE mRNA in the HCV-infected cells decreased gradually and showed a sharp drop between 48 and 60 h pi (Fig. 3C), and the amount of apoE protein in the HCV-infected cells and culture media showed similar patterns to that of apoE mRNA. However, drastic drop of protein levels were observed between 60 and 72 h pi instead of 48–60 h pi (Fig. 3C). This indicates that the decrease of apoE protein in the HCV-infected cells is largely attributed to the decrease of apoE mRNA level. In contrast, there was no significant decrease of the apoE mRNA or protein level in control cells and media through 120 h of cultivation (Fig. 3C and E). Interestingly, the sharp drop in secreted apoE coincided with the decrease of specific infectivity between 60 and 72 h pi (Fig. 3A, B and D). In contrast, the secretion of HCV RNAs into the media increased until 60 h pi and then remained the same through 120 h pi (black line in Fig. 3A). In order to investigate whether the decreased level of apoE protein into cell culture medium was responsible for a decreased specific-infectivity, HCV neutralization experiments were carried out using an apoE-specific antibody. The viruses collected at different stages after infections were treated with an apoE-specific antibody. The viruses collected at various stages were neutralized by the apoE-specific antibody in dosage-dependent manners (Fig. S3). Careful analysis of the data indicated that the virion particles collected at early stage after infection were more sensitive to the neutralizing antibody than those collected at late stage after infection. The data suggest that viruses produced at early stage after infection rely on the apoE-dependent infection process more than those produced at late stage after infection thus show higher infectivity. The data also suggest that the infectious virion particles collected at the late stage of infection also contain some apoE proteins, and that the late stage of infections are, at least in part, facilitated by apoE. These results indicate that the secretion of apoE is likely related with the production of infectious virion particles but not with the secretion of HCV RNA-containing particles and that the composition of virion particles may change during HCV infection cycle.

Characterization of HCV virion particles produced at different stage after infection

Previous studies had revealed that the HCV RNA-containing particles produced in cell culture display a broad range of buoyant densities, suggesting the existence of HCV virions with different components (Hijikata et al., 1993; Pumeechockchai et al., 2002). The authors used mixtures of HCV particles produced at various stages of infection. To investigate the properties of HCV particles produced at specific stages of infection, we harvested the culture media of HCV-infected cells every 12 h and analyzed the samples by isopycnic sucrose density gradient. The amounts of HCV RNAs in each fraction of sucrose gradient were quantified by RT-qPCR, the titers of infectious HCV particles in each fraction were determined by infection of naïve Huh7.5.1 cells (Fig. 4). The majority of viral RNAs were fractionated at buoyant densities between 1.15 and 1.17 g/ml throughout the infection course (black lines in Fig. 4A–C). Although the high buoyant density fractions contained the highest amounts of viral RNA, only low levels of infectious viruses were found in these fractions. This indicates that most of the viral RNAs in the high density fractions are not infectious. The fraction containing the highest titer of infectious HCV was the lowest buoyant density fraction (<1.05 g/ml) from an early stage of infection (36 h pi) (gray line in Fig. 4A). The infectivity of HCV gradually decreased as time passed by (Fig. 4). Noticeably, the highest infectivity fractions shifted toward the higher density fractions as infection proceeded (1.05 g/ml at 36 h pi, 1.12 g/ml at 72 h pi and 1.14 g/ml at 108 h pi) (gray line in Fig. 4). A similar trend of viral production was clearly observed when we analyzed the data in terms of percentiles of infectious virus dose and the amount of viral RNA in each fraction (Fig. S4). This indicates that highly infectious virion particles of very low buoyant density (<1.05 g/ml) are produced early in the infective process (36 h pi), whereas a large quantity of poorly infectious virion particles with high buoyant densities are shed from the infected cells thereafter.

Discussion

We herein monitored HCV proliferation in a cell culture system through synchronous infection of high titer viruses and obtained a one-step growth curve for HCV for the first time. During HCV proliferation, the quantities of positive- and

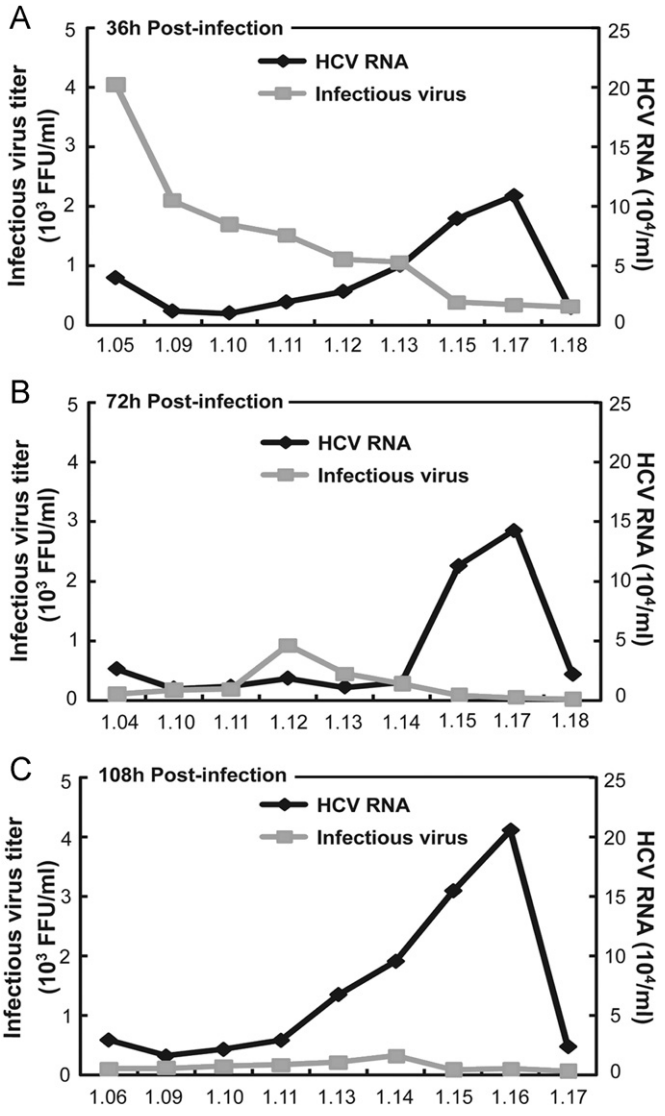

Fig. 4. Characterization of HCV virion particles produced at different times after infection. Huh7.5.1 cells inoculated with HCVcc at a MOI of ~6 FFU/cell were cultivated with complete DMEM. The culture media were harvested every 12 h and replaced with fresh media. Culture media were harvested at 36 h (A), 72 h (B), and 108 h (C) after HCV infection and concentrated to 1 ml with a Vivaspin (100-kD cut-off). The concentrated culture media were subjected to 20–60% sucrose density gradient centrifugation, and samples were collected from top to bottom. The infectious virus titer (10^3 FFU/ml, gray line), HCV RNA (10^4/ml, black line) are shown (A–C).

negative-strand viral RNAs were measured, and infectivity and virion compositions were compared.

After the attachment of HCV onto cells, a sharp drop of cell-associated level was observed at the very early stage of infection (6 h pi). The production of negative-strand RNA was first detected at 6 h pi, and synthesis was biased toward negative-strand RNAs until 9 h pi, when the molar ratio of positive- to negative-strand RNA was around 1:1. This may indicate that almost all viral RNAs at this stage (9 h pi) were the double-stranded RNAs called the 'replicative intermediate' (Chang et al., 2000). The ratio of viral RNAs remained 1:1 until 12 h pi, even though the copy number of viral RNAs almost doubled from 9 h pi to 12 h pi. After this stage, biased synthesis of positive-strand RNAs occurred, until the ratio of positive- to negative-strand RNA exceeded 100:1 at 120 h pi. During this period (24 h to 120 h pi), it is likely that multiple rounds of positive-strand RNA synthesis occurred from a single template of negative-strand RNA, and new positive- strand RNA syntheses may have commenced before completion of the prior round, as seen in the syntheses of picornaviral RNAs (Belsham and Normann, 2008).The HCV-infected cell has higher ratio of positive- to negative-strand RNA than subgenomic and full-length replicons which have the ratio of less than 10. We can speculate plausible reasons for this discrepancy. (1) The optimization of replicons, which has only replication and translation steps of virus life cycle, may result in less production of positive-sense RNAs. That is, mass production of positive-sense RNA to be encapsidated into virion particles is not needed for the maintenance of replicon in cells. (2) The infectious HCV clone JFH-1 was originated from a patient with fulminant hepatitis that is caused by robust proliferation of HCV (Kato et al., 2007). Further investigations will be needed to confirm these speculations.

Infectious viruses were detected in the media at 12 h pi (Fig. 2A) suggesting that the latent period of HCV is about 12 h. To our knowledge, this is the first report describing the latent period of HCV. The cumulative titer of infectious HCV increased until 60 h pi in both cell-associated and secreted viruses, and decreased gradually thereafter (Fig. 2A).These kinetics of infectious HCV production are similar to those reported previously by Deborah et al. (Song et al., 2010). Here, we also monitored the production of infectious virion particles over time, by harvesting and changing the medium every 12 h after infection (Fig. 3A). The secretion of infectious viruses increased until 60 h pi and then precipitately decreased (gray line in Fig. 3A). In contrast, the secreted HCV RNAs reached their highest level at 60 h pi and remained high until 120 h pi (black line in Fig. 3A). The viral RNAs, which are not encapsidated but resistant to RNase A, were also included in calculating the amount of secreted HCV RNAs since there is no suitable experimental method to discriminate the encapsidated virion RNAs from unencapsidated but RNase-resistant RNAs that are likely to exist in exosomes. Considering all of RNase-resistant viral RNAs as variants of virion particles, the specific infectivity of HCV was high during the early stage of infection (12 to 60 h pi), and thereafter decreased 10- to 100-fold during the later stages of infection (72 to 108 h pi) (Fig. 3B).

Previous studies showed that apoE is required for the formation of infectious HCV particles (Gastaminza et al., 2008; Huang et al., 2007; Nahmias et al., 2008). However, the levels of apoE inside and/or outside of HCV-infected cells during the infection cycle have not been reported. We found that apoE protein levels were much lower both inside and outside the HCV-infected cells at the late stage of infection (Fig. 3D). In control cells, the amounts of intracellular and secreted apoE remained unchanged through 120 h (Fig. 3E). The apoE mRNA levels were significantly decreased after 60 h pi (Fig. 3C), at which HCV-infected cells do not show cytotoxicity (Fig. 2E). The levels of ApoE protein inside and outside of the HCV-infected cells precipitately decreased in following 12 h, that is, 72 h pi (Fig. 3D). This indicates that the reduction of apoE protein level is largely attributed to the reduction of apoE mRNA level. However, the molecular basis of the modulation of apoE mRNA level in HCV-infected cells remains to be elucidated. It is plausible that the virion particles produced at the early stage of infection (12 to 60 h pi) are associated with larger amounts of apoE proteins than those produced at the late stage of infection, which results in the difference of specific infectivity of HCV during the infection cycle. This result is supported by a recent report showing that apoE proteins reside on the surface of infectious virion particles (Merz et al., 2011). However, the content of apoE may not be the sole reason of the change of HCV infectivity. Other viral or cellular protein(s) may also contribute to the change in specific infectivity of HCV during the infection cycle. Further researches are needed to understand the molecular details of the virus infectivity change.

Several studies have suggested that the virion particles with low density have higher infectivity. Moreover, it was found that the low-density HCV particles were detected more often in acute infection, while high-density HCV particles were detected more often in chronic infection in patients (Pumeechockchai et al., 2002; Watson et al., 1996). However, the basis for this phenomenon is not yet clearly understood. Here, we report that virus particles produced during the early stages of infection are more infectious and have a very low buoyant density (1.05 g/ml). As the infection progresses, the peak of infectious virus particles shifts toward the higher-density fractions (Fig. 4). The difference of buoyant density among the HCV particles during the proliferation cycle might be responsible for the heterogeneity of HCV particles in HCV patients (Carrick et al., 1992; Kanto et al., 1994; Miyamoto et al., 1992), and for the changes of infectivity and buoyant densities during the pathogenic course of HCV (Pumeechockchai et al., 2002; Watson et al., 1996). Thus, acutely infected patients experience active new infections that produce low-density, highly infectious HCV particles. In contrast, chronically infected patients experience fewer new infections and HCV-infected cells at the late stage of infection dominate the population, resulting in the production of high-density, poorly infectious HCV particles.

Conclusions

The one-step growth curve shown herein provides a foundation for understanding the steps of HCV replication and the production of various HCV particles during the proliferation cycle. Additional investigations into the pathogenic relevance of the changes in HCV infectivity and composition during the proliferation cycle will shed new light on the pathogenesis of HCV in patients.

Materials and methods

Cell line and cell culture

The human hepatoma cell line, Huh7.5.1 (Zhong et al., 2005), was grown in Dulbecco's modified Eagle's medium (DMEM; Gibco) supplemented with antibiotics (100 U/ml penicillin, 10 μg/ml streptomycin) and 10% fetal bovine serum (Hyclone) at 37 °C in a humidified 5% CO_2 environment.

Viral production and concentration

In vitro transcription and RNA electroporation were performed as previously described (Wakita et al., 2005). Approximately 3×10^6 Huh7.5.1 cells were electroporated with in vitro-transcribed RNAs derived from JFH1 containing the cell culture–adapted virus in the E2 and p7 protein (Kim et al., 2011). Cell culture media were collected 3–5 day after electroporation, and naïve Huh7.5.1 cells were infected with the generated viruses. The cell culture media of infected cells were collected 3–5 day post infection. The HCV-containing cell culture media were then filtered with a 0.45 μm and the filtrates were concentrated with a Vivaspin (Millipore; 100-kD cut-off). The concentrated HCV culture medium was loaded onto a 20% sucrose cushion, and HCV particles were collected by ultracentrifugation at 4 °C for 4 h at 27,000 rpm (SW48 rotor; Beckman). The viral pellet was resuspended with complete medium (Chang et al., 2007).

Measurement of infectious virus titer

The infectivity titer was determined on Huh7.5.1 cells by end-point dilution followed by immunofluorescence, as previously described (Zhong et al., 2005). Briefly, the virus stock was subjected to 10-fold serial dilutions, and naïve Huh7.5.1 cells were infected with diluted virus for 3 h. After infection, the cells were washed with PBS and overlain with complete DMEM containing GUM tragacanth (Sigma) to prevent secondary infection (Kedmi and Katzenelson, 1978; Okuno et al., 1990). At 72 h after infection, the cells were fixed with 3% paraformaldehyde, permeabilized with 0.1% Triton X-100 and incubated with a monoclonal anti-core antibody (Thermo Scientific; 1:400 dilution). The core-expressing cells were visualized using Alexa Fluor 488-conjugated donkey anti-mouse IgG (Invitrogen, 1:200 dilution). Infectivity titers were expressed as the number of infection focus-forming units per ml (FFU/ml).

Cytotoxicity assay

We used a ToxiLight bioassay kit (Lonza) to measure the release of adenylate kinase (AK) following the loss of cell membrane integrity. Culture media were harvested at the indicated times, samples were incubated for 5 min with the AK detection reagent, and the results were detected using a luminescence reader (Crouch et al., 1993; Niles et al., 2009).

Preparation of cell-associated and secreted RNAs, and quantification of RNAs by real-time RT-PCR

Cell culture supernatants harvested from infected Huh7.5.1 cells were treated with RNase A solution (final concentration, 40 μg/ml) for 30 min at 37 °C, as previously described (Gastaminza et al., 2006). Cellular RNAs were isolated using the TRIzol reagent (Invitrogen), and HCV RNAs were isolated from culture supernatants using the TRIzol LS reagent (Invitrogen). From these samples, cDNAs were synthesized using Improm II reverse transcriptase (Promega), and SYBR green qPCR was performed using a Light Cycles 2 system (Roche). HCV transcript levels were determined by comparison to standard curves derived from serially diluted JFH1 plasmid. Quantitative real-time RT-PCR (RT-qPCR) analysis of the HCV genome was performed using primers specific for JFH1, as previously described (Kumthip et al., 2012; Zhong et al., 2005). A pair of PCR primers (HCV-R 5′-TCAGGCAGTACCACAAGGC-3′, HCV-F 5′-TCTGCGGAACCGGTGAGTA-3′) was used to monitor positive- and negative- strand HCV RNAs.

Western blot analysis

HCV-infected cell lysates were prepared, and protein concentrations were determined using a protein assay reagent (Thermo Scientific). HCV-infected cell lysates were resolved by 13.5% sodium dodecyl sulfate–polyacrylamide gel electrophoresis (SDS-PAGE), and transferred onto a nitrocellulose membrane. Western blotting was performed using core-, E2-, and GAPDH-specific antibodies. The antibodies against core and E2 (AP 33) were kindly provided by Ralf Bartenschlager (University of Heidelberg) and Arvind Patel (University of Glasgow), respectively. The antibody against GAPDH was purchased from SeroTec. To quantify the amount of secreted apoE, 25 μl of cell culture medium was resolved by 10% SDS-PAGE, and the level of apoE was monitored by Western blotting using an apoE-specific antibody (Calbiochem).

Isopycnic sucrose density gradients analysis

Cell culture supernatants were collected at the indicated times and concentrated 10-fold with a Vivaspin (100-kD cut-off). The concentrated supernatants were then loaded on the top of a 20–60% sucrose gradient prepared in TNE buffer (100 mM NaCl, 10 mM Tris–HCl, and 1 mM EDTA), which was centrifuged at 40,000 rpm and 4 °C for 16 h in a SW41 rotor (Beckman), as previously described (Cai et al., 2005). A total of 12 fractions (1 ml each) were collected from the top to the bottom of the sucrose gradient. The sucrose in each fraction was diluted by adding 10 ml of PBS, and the virion particles were precipitated by ultracentrifugation at 40,000 rpm and 4 °C for 16 h in a SW41 rotor (Beckman). The resulting pellet was resuspended with 1 ml of serum-free DMEM. The HCV RNAs in each fraction (250 μl) were extracted with TRIzol LS reagent and quantified by RT-qPCR. The infectivity of HCV virions in each fraction was determined by inoculating Huh7.5.1 cells with 200 μl of resuspended sample from each fraction.

Production of synthetic HCV RNA

The region corresponding to 5′UTR-NS2 of JFH was cloned into the NotI/EcoRI sites of plasmid pSK(−) vector. Positive- and negative-strand HCV RNAs were synthesized by in vitro transcription with T7 and T3 RNA polymerases, respectively. The DNA templates in the transcription reactions were digested with DNase I (Ambion), and the concentration of RNA was adjusted to 1×10^{11} copies/μl.

Observation of effect of an apoE-specific antibody on HCV infectivity

Culture media harvested at the indicated times was incubated with increasing concentrations (0, 0.4, 2, 10, and 50 μg/ml) of an apoE antibody (Calbiochem) (Merz et al., 2011; Owen et al., 2009) or a negative control goat IgG (Santa Cruz) antibody at room temperature for 1 h. The antibody-treated culture media were used in measuring infectious HCV titers.

Acknowledgments

This research was supported by the World Class University (WCU) Program (No. R31-10105), and the BRL (No. 2010-0019706) through the National Research Foundation funded by the Ministry of Education, Science and Technology. We are grateful to Ralf Bartenschlager (University of Heidelberg) for the core antibody, Arvind Patel (University of Glasgow) for the E2 antibody, Francis Chisari (Scripps Research Institute) for the Huh 7.5.1 cell line and Takaji Wakita (National Institute of Infectious Disease, Tokyo, Japan).

Appendix A. Supplementary information

Supplementary data associated with this article can be found in the online version at http://dx.doi.org/10.1016/j.virol.2012.08.046.

References

Aizaki, H., Lee, K.J., Sung, V.M., Ishiko, H., Lai, M.M., 2004. Characterization of the hepatitis C virus RNA replication complex associated with lipid rafts. Virology 324 (2), 450–461.

Ali, N., Tardif, K.D., Siddiqui, A., 2002. Cell-free replication of the hepatitis C virus subgenomic replicon. J. Virol. 76 (23), 12001–12007.

Andre, P., Komurian-Pradel, F., Deforges, S., Perret, M., Berland, J.L., Sodoyer, M., Pol, S., Brechot, C., Paranhos-Baccala, G., Lotteau, V., 2002. Characterization of low- and very-low-density hepatitis C virus RNA-containing particles. J. Virol. 76 (14), 6919–6928.

Bartenschlager, R., Lohmann, V., 2001. Novel cell culture systems for the hepatitis C virus. Antiviral Res. 52 (1), 1–17.

Belsham, G.J., Normann, P., 2008. Dynamics of picornavirus RNA replication within infected cells. J. Gen. Virol. 89 (Pt 2), 485–493.

Benga, W.J., Krieger, S.E., Dimitrova, M., Zeisel, M.B., Parnot, M., Lupberger, J., Hildt, E., Luo, G., McLauchlan, J., Baumert, T.F., Schuster, C., 2010. Apolipoprotein E interacts with hepatitis C virus nonstructural protein 5A and determines assembly of infectious particles. Hepatology 51 (1), 43–53.

Bessaud, M., Autret, A., Jegouic, S., Balanant, J., Joffret, M.L., Delpeyroux, F., 2008. Development of a Taqman RT-PCR assay for the detection and quantification of negatively stranded RNA of human enteroviruses: evidence for false-priming and improvement by tagged RT-PCR. J. Virol. Methods 153 (2), 182–189.

Boncristiani, H.F., Rossi, R.D., Criado, M.F., Furtado, F.M., Arruda, E., 2009. Magnetic purification of biotinylated cDNA removes false priming and ensures strand-specificity of RT-PCR for enteroviral RNAs. J. Virol. Methods 161 (1), 147–153.

Cai, Z., Zhang, C., Chang, K.S., Jiang, J., Ahn, B.C., Wakita, T., Liang, T.J., Luo, G., 2005. Robust production of infectious hepatitis C virus (HCV) from stably HCV cDNA-transfected human hepatoma cells. J. Virol. 79 (22), 13963–13973.

Carabaich, A., Ruvoletto, M., Bernardinello, E., Tono, N., Cavalletto, L., Chemello, L., Gatta, A., Pontisso, P., 2005. Profiles of HCV core protein and viremia in chronic hepatitis C: possible protective role of core antigen in liver damage. J. Med. Virol. 76 (1), 55–60.

Carrick, R.J., Schlauder, G.G., Peterson, D.A., Mushahwar, I.K., 1992. Examination of the buoyant density of hepatitis C virus by the polymerase chain reaction. J. Virol. Methods 39 (3), 279–289.

Chang, K.S., Jiang, J., Cai, Z., Luo, G., 2007. Human apolipoprotein e is required for infectivity and production of hepatitis C virus in cell culture. J. Virol. 81 (24), 13783–13793.

Chang, M., Marquardt, A.P., Wood, B.L., Williams, O., Cotler, S.J., Taylor, S.L., Carithers Jr., R.L., Gretch, D.R., 2000. In situ distribution of hepatitis C virus replicative-intermediate RNA in hepatic tissue and its correlation with liver disease. J. Virol. 74 (2), 944–955.

Craggs, J.K., Ball, J.K., Thomson, B.J., Irving, W.L., Grabowska, A.M., 2001. Development of a strand-specific RT-PCR based assay to detect the replicative form of hepatitis C virus RNA. J. Virol. Methods 94 (1-2), 111–120.

Crouch, S.P., Kozlowski, R., Slater, K.J., Fletcher, J., 1993. The use of ATP bioluminescence as a measure of cell proliferation and cytotoxicity. J. Immunol. Methods 160 (1), 81–88.

El-Hage, N., Luo, G., 2003. Replication of hepatitis C virus RNA occurs in a membrane-bound replication complex containing nonstructural viral proteins and RNA. J. Gen. Virol. 84 (Pt 10), 2761–2769.

Gastaminza, P., Cheng, G., Wieland, S., Zhong, J., Liao, W., Chisari, F.V., 2008. Cellular determinants of hepatitis C virus assembly, maturation, degradation, and secretion. J. Virol. 82 (5), 2120–2129.

Gastaminza, P., Dryden, K., Boyd, B., Wood, M., Law, M., Yeager, M., Chisari, F.V., 2010. Ultrastructural and biophysical characterization of hepatitis C virus particles produced in cell culture. J. Virol..

Gastaminza, P., Kapadia, S.B., Chisari, F.V., 2006. Differential biophysical properties of infectious intracellular and secreted hepatitis C virus particles. J. Virol. 80 (22), 11074–11081.

Grove, J., Nielsen, S., Zhong, J., Bassendine, M.F., Drummer, H.E., Balfe, P., McKeating, J.A., 2008. Identification of a residue in hepatitis C virus E2 glycoprotein that determines scavenger receptor BI and CD81 receptor dependency and sensitivity to neutralizing antibodies. J. Virol. 82 (24), 12020–12029.

Hardy, R.W., Marcotrigiano, J., Blight, K.J., Majors, J.E., Rice, C.M., 2003. Hepatitis C virus RNA synthesis in a cell-free system isolated from replicon-containing hepatoma cells. J. Virol. 77 (3), 2029–2037.

Hijikata, M., Shimizu, Y.K., Kato, H., Iwamoto, A., Shih, J.W., Alter, H.J., Purcell, R.H., Yoshikura, H., 1993. Equilibrium centrifugation studies of hepatitis C virus: evidence for circulating immune complexes. J. Virol. 67 (4), 1953–1958.

Hishiki, T., Shimizu, Y., Tobita, R., Sugiyama, K., Ogawa, K., Funami, K., Ohsaki, Y., Fujimoto, T., Takaku, H., Wakita, T., Baumert, T.F., Miyanari, Y., Shimotohno, K., 2010. Infectivity of hepatitis C virus is influenced by association with apolipoprotein E isoforms. J. Virol. 84 (22), 12048–12057.

Huang, H., Sun, F., Owen, D.M., Li, W., Chen, Y., Gale Jr., M., Ye, J., 2007. Hepatitis C virus production by human hepatocytes dependent on assembly and secretion of very low-density lipoproteins. Proc. Nat. Acad. Sci. U.S.A. 104 (14), 5848–5853.

Jiang, J., Luo, G., 2009. Apolipoprotein E but not B is required for the formation of infectious hepatitis C virus particles. J. Virol. 83 (24), 12680–12691.

Kanto, T., Hayashi, N., Takehara, T., Hagiwara, H., Mita, E., Naito, M., Kasahara, A., Fusamoto, H., Kamada, T., 1994. Buoyant density of hepatitis C virus recovered from infected hosts: two different features in sucrose equilibrium density-gradient centrifugation related to degree of liver inflammation. Hepatology 19 (2), 296–302.

Kato, T., Matsumura, T., Heller, T., Saito, S., Sapp, R.K., Murthy, K., Wakita, T., Liang, T.J., 2007. Production of infectious hepatitis C virus of various genotypes in cell cultures. J. Virol. 81 (9), 4405–4411.

Kedmi, S., Katzenelson, E., 1978. A rapid quantitative fluorescent antibody assay of polioviruses using tragacanth gum. Arch. Virol. 56 (4), 337–340.

Kim, C.S., Keum, S.J., Jang, S.K., 2011. Generation of a cell culture–adapted hepatitis C virus with longer half life at physiological temperature. PLoS One 6 (8), e22808.

Kumthip, K., Chusri, P., Jilg, N., Zhao, L., Fusco, D.N., Zhao, H., Goto, K., Cheng, D., Schaefer, E.A., Zhang, L., Pantip, C., Thongsawat, S., O'Brien, A., Peng, L.F., Maneekarn, N., Chung, R.T., Lin, W., 2012. Hepatitis C virus NS5A disrupts STAT1 phosphorylation and suppresses type I Interferon signaling. J. Virol. 86 (16), 8581–8591.

Lai, V.C., Dempsey, S., Lau, J.Y., Hong, Z., Zhong, W., 2003. In vitro RNA replication directed by replicase complexes isolated from the subgenomic replicon cells of hepatitis C virus. J. Virol. 77 (3), 2295–2300.

Lanford, R.E., Chavez, D., Chisari, F.V., Sureau, C., 1995. Lack of detection of negative-strand hepatitis C virus RNA in peripheral blood mononuclear cells and other extrahepatic tissues by the highly strand-specific rTth reverse transcriptase PCR. J. Virol. 69 (12), 8079–8083.

Liang, T.J., Jeffers, L.J., Reddy, K.R., De Medina, M., Parker, I.T., Cheinquer, H., Idrovo, V., Rabassa, A., Schiff, E.R., 1993. Viral pathogenesis of hepatocellular carcinoma in the United States. Hepatology 18 (6), 1326–1333.

Lindenbach, B.D., Evans, M.J., Syder, A.J., Wolk, B., Tellinghuisen, T.L., Liu, C.C., Maruyama, T., Hynes, R.O., Burton, D.R., McKeating, J.A., Rice, C.M., 2005. Complete replication of hepatitis C virus in cell culture. Science 309 (5734), 623–626.

Lindenbach, B.D., Meuleman, P., Ploss, A., Vanwolleghem, T., Syder, A.J., McKeating, J.A., Lanford, R.E., Feinstone, S.M., Major, M.E., Leroux-Roels, G., Rice, C.M., 2006. Cell culture-grown hepatitis C virus is infectious in vivo and can be recultured in vitro. Proc. Nat. Acad. Sci. U.S.A. 103 (10), 3805–3809.

Lindenbach, B.D., Rice, C.M., 1997. Trans-complementation of yellow fever virus NS1 reveals a role in early RNA replication. J. Virol. 71 (12), 9608–9617.

Lohmann, V., Korner, F., Koch, J., Herian, U., Theilmann, L., Bartenschlager, R., 1999. Replication of subgenomic hepatitis C virus RNAs in a hepatoma cell line. Science 285 (5424), 110–113.

Merz, A., Long, G., Hiet, M.S., Brugger, B., Chlanda, P., Andre, P., Wieland, F., Krijnse-Locker, J., Bartenschlager, R., 2011. Biochemical and morphological properties of hepatitis C virus particles and determination of their lipidome. J. Biol. Chem. 286 (4), 3018–3032.

Miyamoto, H., Okamoto, H., Sato, K., Tanaka, T., Mishiro, S., 1992. Extraordinarily low density of hepatitis C virus estimated by sucrose density gradient centrifugation and the polymerase chain reaction. J. Gen. Virol. 73 (Pt 3), 715–718.

Nahmias, Y., Goldwasser, J., Casali, M., van Poll, D., Wakita, T., Chung, R.T., Yarmush, M.L., 2008. Apolipoprotein B-dependent hepatitis C virus secretion is inhibited by the grapefruit flavonoid naringenin. Hepatology 47 (5), 1437–1445.

Nielsen, S.U., Bassendine, M.F., Burt, A.D., Martin, C., Pumeechockchai, W., Toms, G.L., 2006. Association between hepatitis C virus and very-low-density lipoprotein (VLDL)/LDL analyzed in iodixanol density gradients. J. Virol. 80 (5), 2418–2428.

Niles, A.L., Moravec, R.A., Riss, T.L., 2009. In vitro viability and cytotoxicity testing and same-well multi-parametric combinations for high throughput screening. Curr. Chem. Genomics 3, 33–41.

Okuno, Y., Tanaka, K., Baba, K., Maeda, A., Kunita, N., Ueda, S., 1990. Rapid focus reduction neutralization test of influenza A and B viruses in microtiter system. J. Clin. Microbiol. 28 (6), 1308–1313.

Owen, D.M., Huang, H., Ye, J., Gale Jr., M., 2009. Apolipoprotein E on hepatitis C virion facilitates infection through interaction with low-density lipoprotein receptor. Virology 394 (1), 99–108.

Pumeechockchai, W., Bevitt, D., Agarwal, K., Petropoulou, T., Langer, B.C., Belohradsky, B., Bassendine, M.F., Toms, G.L., 2002. Hepatitis C virus particles of different density in the blood of chronically infected immunocompetent and immunodeficient patients: Implications for virus clearance by antibody. J. Med. Virol. 68 (3), 335–342.

Quinkert, D., Bartenschlager, R., Lohmann, V., 2005. Quantitative analysis of the hepatitis C virus replication complex. J. Virol. 79 (21), 13594–13605.

Song, H., Li, J., Shi, S., Yan, L., Zhuang, H., Li, K., 2010. Thermal stability and inactivation of hepatitis C virus grown in cell culture. Virol. J. 7, 40.

Tscherne, D.M., Evans, M.J., von Hahn, T., Jones, C.T., Stamataki, Z., McKeating, J.A., Lindenbach, B.D., Rice, C.M., 2007. Superinfection exclusion in cells infected with hepatitis C virus. J. Virol. 81 (8), 3693–3703.

Wakita, T., Pietschmann, T., Kato, T., Date, T., Miyamoto, M., Zhao, Z., Murthy, K., Habermann, A., Krausslich, H.G., Mizokami, M., Bartenschlager, R., Liang, T.J., 2005. Production of infectious hepatitis C virus in tissue culture from a cloned viral genome. Nat. Med. 11 (7), 791–796.

Wasley, A., Alter, M.J., 2000. Epidemiology of hepatitis C: geographic differences and temporal trends. Semin. Liver Dis. 20 (1), 1–16.

Watson, J.P., Bevitt, D.J., Spickett, G.P., Toms, G.L., Bassendine, M.F., 1996. Hepatitis C virus density heterogeneity and viral titre in acute and chronic infection: a comparison of immunodeficient and immunocompetent patients. J. Hepatol. 25 (5), 599–607.

Zhong, J., Gastaminza, P., Cheng, G., Kapadia, S., Kato, T., Burton, D.R., Wieland, S.F., Uprichard, S.L., Wakita, T., Chisari, F.V., 2005. Robust hepatitis C virus infection in vitro. Proc. Nat. Acad. Sci. U.S.A. 102 (26), 9294–9299.